PALEOLAKE DEPOSITS ON MARS: PERSPECTIVES ON SOURCE-TO-SINK MINERALOGY FROM LAKE TOWUTI, INDONESIA. T. A. Goudge[1], J. F. Mustard[1], J. M. Russell[1], and J. W. Head[1], [1]Dept. of Earth, Environmental and Planetary Sciences, Brown University, Box 1846 Providence, RI 02912. (Contact: Tim_Goudge@brown.edu)

Introduction: Ancient paleolake basins are amongst the best evidence for surface fluvial activity early in martian history [e.g., *1-3*]. Many of these paleolakes contain sedimentary deposits formed when there was standing water within the basin [e.g., *1,2,4*]. Study of lacustrine sedimentary deposits on Earth can provide fundamental constraints on martian paleolake deposits, which are largely restricted to remote sensing analyses. To provide perspective on how remote sensing data can be used to study lacustrine sediment, we have studied the source-to-sink mineralogy of Lake Towuti, a modern terrestrial lake, using visible to near-infrared (VNIR) reflectance spectroscopy as the primary dataset. Our results may also aid in the interpretation of combined *in situ* and remote sensing data for Gale crater, a closed-basin paleolake [*2*,*5*] and the site of exploration for the Mars Science Laboratory (MSL).

Lake Towuti is a large (area = ~560 km^2), hydrologically open lake on the island of Sulawesi, Indonesia [*6,7*]. The ~1280 km^2 catchment area is largely composed of lateritic soils derived from, and overlain on, the ultramafic East Sulawesi Ophiolite [*8,9*], compositionally comparable to the basaltic martian crust [*10,11*]. We analyzed the bedload and suspended load (source sediment) from the Mahalona River, the primary input to Lake Towuti, and a piston core (sink sediment) from the distal margins of a delta deposit at the mouth of this river.

Methods: *Input Sediment.* Bedload samples were freeze-dried and dry sieved to >1 mm, 0.25-1 mm, 63-250 μm, 32-63 μm and <32 μm size fractions. Suspended load samples were freeze-dried, wet sieved to the same size fractions, and freeze-dried again. The reflectance spectra of all 5 size fractions were measured with an Analytical Spectral Devices (ASD) FieldSpec 3 over the wavelength range 350-2500 nm. Major element chemistry of the samples was analyzed using an inductively coupled plasma atomic emission spectrometer (ICP-AES) with flux fusion sample preparation [*12*]. X-ray diffraction (XRD) data were collected using a Bruker D2 PHASER instrument to validate the mineralogy inferred from VNIR spectroscopy

Core. The analyzed core is ~10.5 m in length, and has a basal age of ~20 ka [*7*]. A small, full-length subsection (U-channel) of the core was collected and freeze-dried. Reflectance spectra of this core were measured at 1 cm depth intervals using an ASD FieldSpec 3 attached to a Geotek multisensor core logger. Eleven sub-samples were collected from the core, freeze-dried, and analyzed with the ASD FieldSpec 3, ICP-AES and XRD instruments.

Results: *Input Sediment.* The input sediment samples have a series of distinct spectral absorptions, primarily indicative of phyllosilicate mineralogy (**Fig. 1**). The spectral characteristics are dominated by absorption features of Mg-rich serpentine, including vibrational absorptions centered near ~1390, 2100 and 2320 nm (**Fig. 1**) [*13,14*]. These absorptions are due to the first overtone of the OH stretch (~1390 nm absorption) and a combination tone of the Mg-OH bend and OH stretch (~2320 nm absorption) [*13,14*]. The absorption centered near ~2100 nm is characteristic of serpentine; however, its cause is not fully understood, although it is likely to be related to Mg-OH vibrational modes [*14*]. The input sediment spectra also have a strong absorption feature centered near ~1900 nm, caused by a combination tone of OH stretch and H-O-H bend from structural H_2O [*14*]. The dominance of serpentine in the input sediment is also confirmed with XRD data.

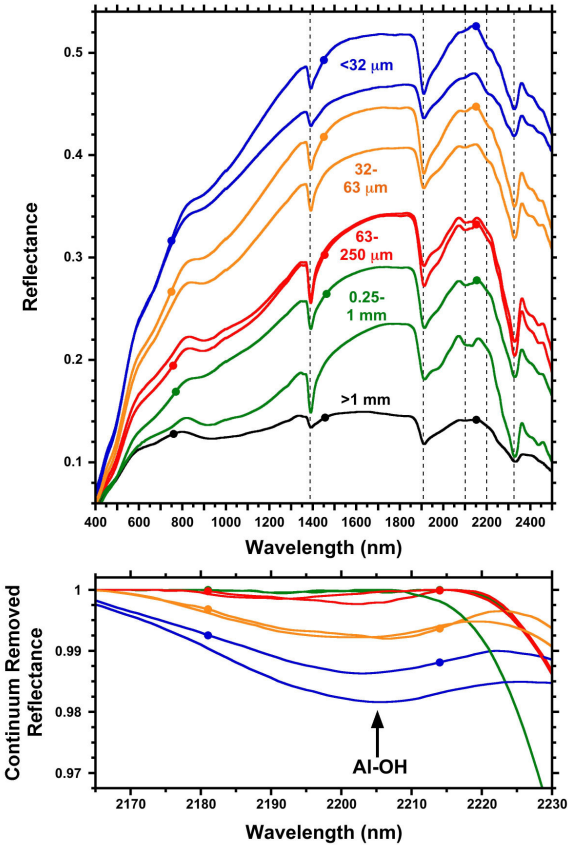

Figure 1. *Grain size fraction spectra for bedload (lines with dots) and suspended load (solid lines) input sediment. Top plot shows reflectance with dashed lines at ~1390, 1910, 2100, 2200, and 2320 nm. Bottom plot shows continuum-removed reflectance with the same color coding as the top plot.*

While all of the input sediment is spectrally dominated by serpentine (**Fig. 1**), there are subtle changes in the spectra of the different size fractions. Specifically, in the smallest grain size fractions, there is a subtle absorption centered near ~2200 nm (**Fig. 1**). This ~2200 nm absorption is due to a combination of the Al-OH bend and OH stretch within an Al-bearing phyllosilicate, such as kaolinite or montmorillonite [*14,15*]. These results are confirmed by major

element chemistry, which shows increasing Al_2O_3 content with decreasing grain size (**Fig. 2**), and XRD data that identify increased kaolinite proportions in the smallest grain size fraction samples.

The shape of the ~1900 nm absorption feature also changes noticeably with grain size. The largest grain size fractions exhibit a broader, 'boxy' ~1900 nm absorption feature, while the smallest grain size fractions exhibit a narrower, more asymmetric ~1900 nm absorption feature (**Fig. 1**). We quantified this change with the spectral parameter BD1975:BD1916, which takes the ratio of the band depth at 1975 nm to the band depth at 1916 nm. The narrower, and more asymmetric the ~1900 nm absorption feature, the lower the BD1975:BD1916 value, as shown in a plot of grain size versus BD1975:BD1916 (**Fig. 2**).

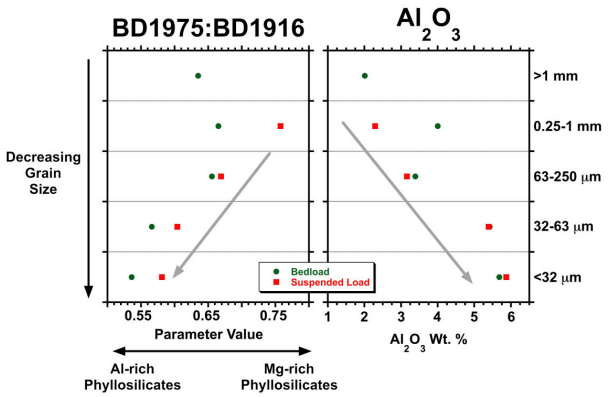

Figure 2. *Grain size versus BD1975:BD1916 ratio (left plot) and Al_2O_3 content (right plot) for the input sediment.*

Core. Spectra from the sediment core show similar overall characteristics to the input sediment. In applying the BD1975:BD1916 parameter to the >1000 spectra from the core, there are clear, systematic changes in the downcore spectral signature (**Fig. 3**). This plot shows both high frequency variations in BD1975:BD1916, as well as a long-term trend for the sediment core (**Fig. 3**).

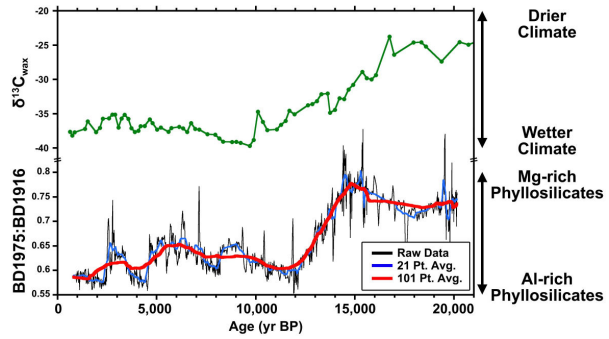

Figure 3. *Biogeochemical precipitation proxy ($\delta^{13}C$ of leaf waxes in Lake Towuti sediment cores; top plot) [7] and BD1975:BD1916 parameter value (bottom plot) for the analyzed lake sediment core versus time. Note the similar structure in the two records.*

Discussion: Input sediment from the Mahalona River is spectrally dominated by Mg-rich serpentine (**Fig. 1**), a finding that is confirmed by XRD data. However, there is also a minor spectral contribution from an Al-rich phyllosilicate (kaolinite) that increases with decreasing grain size, seen with VNIR reflectance data (**Fig. 2**). The ICP-AES data show increased Al_2O_3 content coincident with the change in spectral features (**Fig. 2**) and XRD data confirm the presence of kaolinite. Primary variations in the mineralogy of the input river sediment are thus controlled by mineralogic sorting associated with variations in grain size.

This variation in input sediment mineralogy is also recorded in the lake core sediment. The BD1975:BD1916 ratio for the core shows systematic trends (**Fig. 3**), with a period of low values in the modern era (~12-0 ka), preceded by a section of high values from ~20-15 ka (**Fig. 3**). From our analyses of the input sediment spectra (**Figs. 1, 2**), we hypothesize this trend is indicative of a transition from finer material with a larger component of Al-bearing phyllosilicates in the modern era, to coarser material with a larger component of Mg-rich serpentine prior to ~15 ka.

This transition begins at approximately the end of the Last Glacial Maximum (LGM). Precipitation rates in Indonesia were lower during the LGM (**Fig. 3**), and the water level in Lake Towuti dropped [7]. This lake level drop is likely to have exposed coarse, deltaic topset sediment near the mouth of the Mahalona River, and led to progradation of the delta. This would have resulted in delivery of coarser material to the core site, which is currently at the distal margins of this delta. This scenario is wholly consistent with our source-to-sink analysis of this basin.

Conclusions: Our analyses show that VNIR reflectance spectroscopy accurately characterizes the source-to-sink mineralogy of this modern lake system. Major spectral variations in the Lake Towuti sediment are best explained by changes in mineralogy as controlled by the grain size of previously altered input sediment. These results emphasize the importance of grain size dependent mineralogy for the interpretation of VNIR spectroscopy data.

Our results also show that the observed spectral variations within lacustrine sediment of Lake Towuti are consistent with external, paleo-environmental changes that have affected the basin over the past ~20 kyr. We suggest that exposed cross-sections of martian sedimentary deposits should also contain similar paleo-environmental information that is accessible through remote, VNIR reflectance spectroscopy. Future studies of martian paleolake deposits will especially benefit from source-to-sink analyses of mineralogy, as has been done for a handful of martian paleolake systems [e.g., *16,17*].

References: [1] Cabrol, N. and Grin, E. (1999), *Icarus,* **142**:160. [2] Irwin, R., et al. (2005), *JGR*, **110**:E12S15. [3] Fassett, C. and Head, J. (2008), *Icarus,* **198**:37. [4] Goudge, T., et al. (2012), *Icarus,* **219**:211. [5] Grotzinger, J., et al. (2014), *Science,* **343**:1242777-1. [6] Haffner, G., et al. (2001), *The Great Lakes of the World (GLOW): Food-web, health and integrity* (M. Munawar and R. Hecky, Eds.), Blackhuys Publishers, pp. 183-192. [7] Russell, J., et al. (2014), *PNAS,* **111**:5100. [8] Monnier, C., et al. (1995), *Geology,* **23**:851. [9] Kadarusman, A., et al. (2004), *Tectonophysics,* **392**:55. [10] Mustard, J., et al. (2005), *Science,* **307**:1594. [11] McSween, H., et al. (2009), *Science,* **324**:736. [12] Murray, R., et al. (2000), *ODP Tech. Note,* **29**, 27 pp. [13] King, T., and Clark, R. (1989), *JGR,* **94**:13,997. [14] Clark, R., et al. (1990), *JGR,* **95**:12,653. [15] Bishop, J., et al. (2008), *Clay Min.,* **43**:35. [16] Milliken, R., and Bish, D. (2010), *Phil. Mag.,* **90**:2293. [16] Goudge, T., et al. (2014), *LPSC 45,* #1164.